Case Studies in Thermal Engineering 49 (2023) 103373

Contents lists available at ScienceDirect

Case Studies in Thermal Engineering

journal homepage: www.elsevier.com/locate/csite

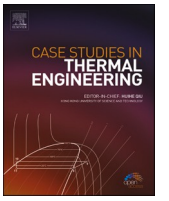

Experimental investigation on cooling performance of vortex tube with rectifier using Taguchi method

Zhuohuan Hu [a], Dan Wang [a], Fan Gao [a], Yan Cao [b], Hongwei Wu [a,c,*]

[a] School of Energy and Power Engineering, University of Shanghai for Science and Technology, 200093, Shanghai, China
[b] Aerospace System Engineering Shanghai, Shanghai, 201109, China
[c] School of Physics, Engineering and Computer Science, University of Hertfordshire, Hatfield, AL10 9AB, UK

ARTICLE INFO

Handling Editor: Huihe Qiu

Keywords:
Taguchi method
Vortex tube
ANOVA
SNR

ABSTRACT

In this article, an experimental study was carried out to investigate the cooling efficiency of a vortex tube equipped with a rectifier utilizing the Taguchi method for analysis. The Coefficient of Performance (COP) was determined as the quality characteristics. In the current study, the inlet pressure, distance between the rectifier and the hot end, the position of the rectifier, the height of the rectifier, the number of blades, the length of blades, the inclination angle of blades with and without ring were selected as the key control factors and levels. Taguchi L18 orthogonal array was applied to design the experiments. The Signal-to-Noise Ratio (SNR), regression, Analysis of Variance (ANOVA) and residual analysis were applied to optimise the combination for COP of the vortex tube. The tests were also conducted to validate the reliability of the predicted optimisation method. Experimental results indicated that: (i) the predicted optimal value falls within a Confidence Interval (CI) of 95%. The analysis also revealed that the length of the blades could be the most influential control factor, accounting for 36.9% of the cooling performance. (ii) the height of the rectifier shows little impact, only contributing 4.7% to the overall cooling performance. (iii) the order of other control factors on COP was inlet pressure (21%), whether the rectifiers with or without ring (12.8%), distance between the rectifier and the hot end (7.9%), the inclination angle of blades (6.2%) and the number of blades (5.3%).

Nomenclature

A	rectifiers with or without ring[-]
COP	coefficient of performance refrigeration[-]
C_p	specific heat at constant pressure[J kg^{-1} $°C^{-1}$]
C_v	specific heat at constant volume[J kg^{-1} $°C^{-1}$]
$C\%$	contribute of each factor[-]
CI	confidence interval[-]
DF_A	freedom degree [−]
DF_T	degree freedom of total[-]
DF_E	degree freedom of error[-]
F	statistical value[-]

* Corresponding author. School of Energy and Power Engineering, University of Shanghai for Science and Technology, 200093, Shanghai, China
E-mail address: h.wu6@herts.ac.uk (H. Wu).

https://doi.org/10.1016/j.csite.2023.103373
Received 29 March 2023; Received in revised form 19 July 2023; Accepted 4 August 2023
Available online 8 August 2023

H	rectifier height [mm]
k	heat capacity[-]
L	blade length [mm]
$\dot{m}$	mass flow rate [kg s^{-1}]
MS	mean square [m^2]
N	blade number[-]
P	pressure [MPa]
Q_c	heat flow [J]
R_g	gas constant [J kg^{-1} k^{-1}]
S	distance between rectifier and hot end [mm]
SS	square deviations number[-]
TSS	total sum of squares[-]
T	temperature [°C]
V_e	error variance[-]
W	Energy [KW]
Y	measured quantity[-]

Greek symbols

α	cold flow ratio[-]
θ	angle [°]
β	regression coefficient[-]
η	number of real repetitions[-]

Subscript

A	A-factor[-]
c	cold air[-]
E/e	due to error[-]
eff	effective[-]
F	the total freedom degree[-]
i	inlet[-]
p	pressure[-]
v	volume[-]

1. Introduction

With the development of science and technology, environmental protection and energy saving has been highly valued and have been attracted wide attention. In the cooling system, it is imperative to enhance its advanced and efficient capabilities [1]. Among the cooling systems, the vortex tube has been extensively studied over the past seven decades. The vortex tube has been widely utilised in various industries in energy and mass separation [2], such as refrigeration, oil and gas industry, aeronautics [3], spot cooling [4] and gas separation due to its long life and excellent separation characteristics [5], which can produce both hot and cold streams of airflows from a highly compressed gas [6,7]. The vortex tube was firstly investigated by the French physicist Georges in 1933 during an experiment with a pump. Afterwards, in 1947, German engineer Rudolf Hilsch modified the vortex tube proposed by Georges J. Ranque's [8,9], therefore the vortex tube is also called Ranque vortex tube, Hilsch vortex tube or Ranque-Hilsch vortex tube [10].

Since then, much effort has been devoted to understanding the behaviour and improvement of the vortex tube [11]. According to the different types of flow modes, vortex tube can be divided into unitary-flow vortex tube and counter-flow vortex tube [12]. The counter-flow vortex tube is a simple structure, which is composed of hot end tube, cold end tube, vortex chamber, a nozzle and a hot end control valve [13]. The high-pressure gas enters tangentially from the nozzle into the vortex chamber, where it expands, rotates at high speed, then forms a swirling flow. The flow field in the vortex tube will have two regions and two outlets. The two regions normally include the core region and the peripheral region. While for the outlet, one outlet is close to the inlet and the other one is at the end of the vortex tube. Due to the axial pressure gradient, the peripheral region of the flow exits from the opening of the valve. The remaining core region of the flow reverts towards the inlet where it is released from the cold end orifice [14].

Vitovsky et al. [15] presented a screw-type vortex generator for energy separation and they investigated the effects of the inlet pressure, pressure at hot and cold outlets of the tube and mass fraction of cold flow in the total flow on the temperature separation. They stated that the flow temperature separation effect could increase with the increase of the inlet pressure. While the flow temperature separation effect would decrease with the outlet pressure is increased. In the review of Kirmaci et al. [16], the working fluid, the number of nozzles, the nozzle structure, the connection mode of the vortex tube and cold mass fraction and other parameters were discussed on the thermal performance of the vortex tube. Their results indicated that the air was the best medium for the vortex tube and the overall highest performance was reached when the number of nozzles was 3 and 4. Suhaimi et al. [17] investigated the performance of vortex tube as a cooling device under different cold mass flow rate and different inlet pressure. It was concluded that

the higher the inlet pressure of the vortex tube, the lower the air temperature, and the higher the cold mass flow rate will be.

In recent years, Taguchi method is widely used to optimise the parameters that affect the energy separation of the vortex tube. Kumar et al. [18] reported a L27 orthogonal array test method to study the effects of the inlet pressure, length of hot tube, inner diameter of hot tube, orifice plate diameter and number of nozzles on hot-outlet air temperature. Analysis of Variance (ANOVA) was utilised to predict the optimal factor levels. Kaya [19] applied a L18 orthogonal array optimisation method to investigate the performance of parallel Ranque-Hilsch Vortex Tube (RHVT) system and determined the control factors and levels. It was found that the order of the influence on the performance of parallel RHVT was: inlet pressure, working fluid, number of nozzles and nozzle material. Gokce [20] employed a Taguchi L16 mix type orthogonal array experiments to determine the influence of the control factors such as the inlet pressure, the connection mode of vortex tube, nozzle material and the number of nozzles on the temperature gradient. The statistical results reported that the ANOVA was within confidence level of 95% and the values of ΔT were mostly influenced by the inlet pressure, followed by connection type, number of orifices and the last is nozzle material. Sarifudin et al. [21] used Taguchi method to estimate the response parameters that affected the cold temperature and refrigeration performance coefficient on the control factors of the vortex tube. The cold end temperature and refrigeration performance coefficient of the vortex tube were predicted. However, it is aforementioned that previous works mainly focus on the investigation of key impact factors such as the number of nozzles, nozzle material, inlet pressure, very little research has been done on the effect caused by the number of rectifiers. In the current work, therefore, several novel rectifiers were designed to organise and optimise the flow field inside the vortex tube, and the optimal rectifier structure is studied in detail by Taguchi method.

In the present work, Taguchi L18 mix type orthogonal array was applied. Three different inlet pressures, three difference rectifier positions and six different types of rectifier structures, including blades length, number of blades, distance between rectifier and the hot end, rectifiers with or without ring, the inclination angle of blades and the height of rectifier, were selected as the control factors to analyze their effect on the COP of the vortex tube in a systematic manner. Residual and regression analysis were performed to seek the optimal combination and determine the quality characteristics of COP, SNR, ANOVA.

2. Experimental method

2.1. Experimental apparatus

Fig. 1 shows the schematic diagram of the experimental apparatus. The apparatus is mainly composed of an air compressor (ZLS05A/8), an air tank, an air dryer (ED-10F), two air filter (T-002), temperature and pressure sensors, a pressure regulating valve and a vortex tube, as illustrated in Fig. 1. The air compressor can produce a maximum pressure of 0.8 Mpa and its maximum power is 50 KW. The air dryer is able to desiccate 1.5 cubic meter air flow per minute and 0.62 KW power will be consumed per hour. The air filter can deal with 2 cubic meter of air to deviate the air flow from water per minute. In the current study, the air will be compressed by the compressor and stored in an air tank. An air filter is arranged at the outlet of the air tank to purify the air flow. Dry air flow can better improve the refrigeration efficiency, therefore, an air dryer is utilised for dehumidification operation. A pressure regulating valve is set to maintain the pressure stability of the air flow and sensors are installed on the tube to measure the mass flow rate. Table 1 listed the parameters of experimental apparatus and measurement instruments.

The structure of the vortex tube used in the current experiment is exhibited in Fig. 2. As shown in Fig. 2(a), the vortex tube is

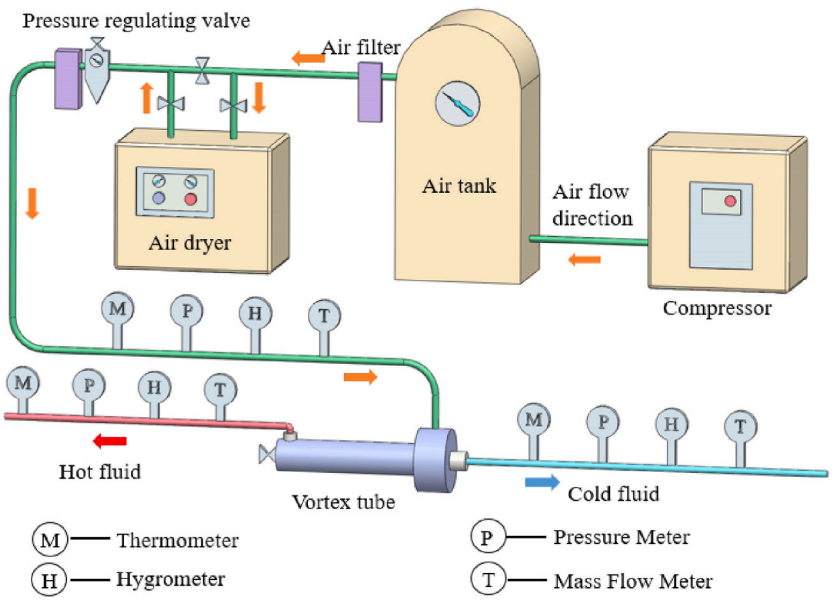

Fig. 1. Schematic diagram of experimental apparatus.

Table 1
Range and uncertainty of equipment used in the experiment.

Instrument	Model	Range	Uncertainty
Air compressor	ZLS05A/8	–	–
Air dryer	ED-10F	–	–
Air filter	T-002	–	–
Pressure meter	CUP-P300	0–0.4Mpa	0.5%
Mass flow meter	FCTMF.E.32.B.S.I.12.DC.J	0.29–289Nm^3	1%
Thermometer	Pt100	−50-100 °C	0.2%
RH&T transmitter	KQ-TH639	0-100%RH	3%
		−20°C-120 °C/	0.3%

composed of an inlet, two outlets (include a cold air outlet and a hot air outlet), a swirl generator and a valve. The function of the valve is to adjust the cold flow ratio. The diagram of the internal device of the vortex tube is demonstrated in Fig. 2(b). The diameter of the pressure inlet D_i is 6 mm, the hot end tube diameter D_h is 10 mm and its length L_h is 200 mm, the rectifier is installed in the hot end tube near the valve. The swirl generator, as shown in Fig. 2(c), has 4 nozzles and the nozzle cross-sectional area is 2 × 2 mm^2. As for the cold end tube, its length L_c is 20 mm and the diameter d_c is 4 mm. The vortex chamber is utilised to hold the swirl generator and its aperture R is 10 mm, as depicted in Fig. 2(d).

It is recognised that the rectifier plays an important role to organise and optimise the flow field inside the vortex tube. In the current study, 18 rectifiers were designed to compare its efficiency. Fig. 3 shows the selected three samples (sample 1, sample 12 and sample 17). Sample 1 is a rectifier without ring and its blade inclination angle is 0°, sample 12 is rectifier with ring and its blade inclination angle is15°, and sample 17 is a rectifier with ring and its blade inclination angle is 30°. The detailed parameters of 18 rectifiers are listed in Table 3.

2.2. Experimental design

Under the condition of the same cold flow ratio (α = 0.5), the influence of the inlet pressure, rectifier structure, and rectifier positions on the vortex tube COP were studied in detail. The control factors and their levels of the design parameters are shown in Table 2.

In the present experiment, the mixed L18 ($2^1 \times 3^6$) array was selected as the orthogonal array. The orthogonal design can greatly reduce the number of the experiments. With traditional full factor experiment method, 1458 times of experiments are needed, while only 18 times of experiments is needed by L18 orthogonal array method. The orthogonal array L18 ($2^1 \times 3^6$), which is consisted of experimental combination of control factors is showed in Table 3.

Where:

L: The Latin square;
18: The number of experimental runs;
2^1: The single factor is classified into two-levels;
3^6: The six factors are classified into three-levels.

3. Taguchi method

3.1. The calculation of COP

COP is a dimensionless number to demonstrate the cooling effect that can be done by a cooler [21]. The temperature difference between the hot and cold ends, cooling and heating flow rate, the volume flow rate at the inlet and outlet, and the density of the hot and cold ends are experimentally obtained. The vortex tube COP value can be calculated based on Eqs. (1)–(6) [22]:

The vortex tube was described as an open system, which can be obtained by the mass conservation:

$$\dot{m}_i = \dot{m}_c + \dot{m}_h \tag{1}$$

where, $\dot{m}_i, \dot{m}_c, \dot{m}_h$ represents the mass flow rate of the vortex tube inlet, the cold outlet and hot outlet, respectively.

Cold flow ratio α indicate the ratio of the mass flow rate at the outlet of the cold end to the mass flow rate at the inlet of vortex tube:

$$\alpha = \frac{\dot{m}_c}{\dot{m}_i} \tag{2}$$

The cooling capacity of vortex tube per unit time:

$$Q_c = \dot{m}_c C_p (T_i - T_c) = \alpha \dot{m}_i C_p (T_i - T_c) \tag{3}$$

The total compression power:

$$W = \dot{m}_i R_g T_i \ln(p_i / p_c) \tag{4}$$

Coefficient of performance (COP):

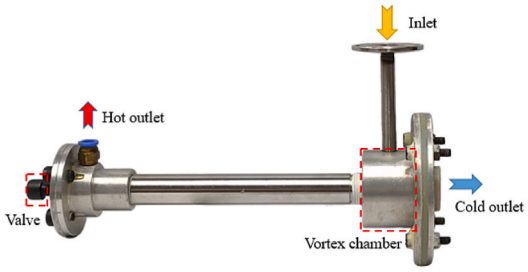

(a) Physical diagram of vortex tube

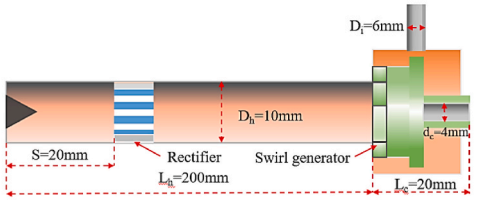

(b) Internal view

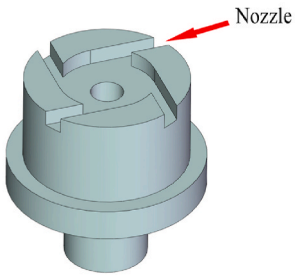

(c) Swirl generator

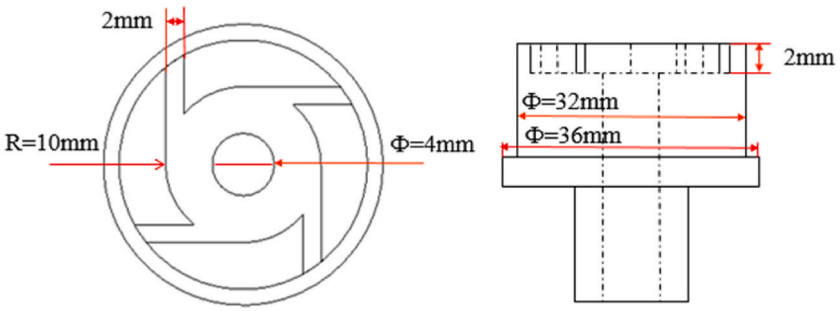

(d) The parameter of swirl generator

Fig. 2. Experimental apparatus of vortex tube.

$$COP = \frac{Q_c}{W} = \frac{C_p}{R_g}\frac{\alpha(T_i - T_c)}{T_i \ln(p_i/p_c)} = \frac{\mathrm{k}}{k-1}\frac{\alpha(T_i - T_c)}{\ln(p_i/p_c)} \tag{5}$$

From the properties of an ideal gas :

$$\frac{C_p}{R_g} = \frac{\mathrm{k}}{k-1}, k = \frac{C_p}{C_v} \tag{6}$$

where, k is the heat capacity of the cold air flow.

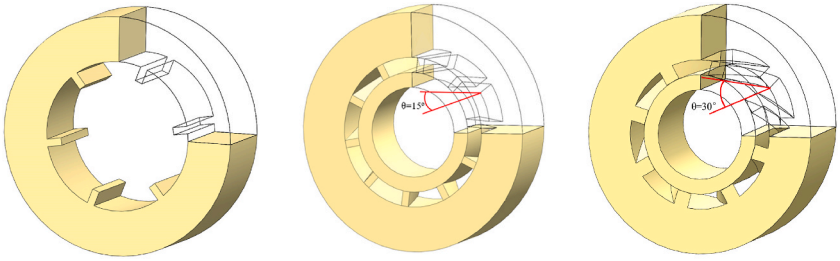

(a) Sample 1 (b) Sample 12 (c) Sample 17

Fig. 3. Structure of rectifiers.

Table 2
Control factors and their levels.

Control factors	Unit	Level 1	Level 2	Level 3
Rectifier with or without ring (A)	–	0	1	
Pressure inlet (P)	MPa	0.3	0.4	0.5
Distance between rectifier and hot end (S)	mm	20	40	60
Blade number (N)	–	6	8	10
Rectifier height (H)	mm	5	10	15
Blade length (L)	mm	1	2	3
Blade inclination angle (θ)	°	0°	15°	30°

Table 3
Orthogonal array of L18 horizontal parameter combination.

Order	A	P (MPa)	S(mm)	N	H(mm)	L(mm)	θ(°)
1	0	0.3	20	6	5	1	0°
2	0	0.4	40	8	10	2	15°
3	0	0.5	60	10	15	3	30°
4	0	0.5	40	6	15	1	15°
5	0	0.3	60	8	5	2	30°
6	0	0.4	20	10	10	3	0°
7	0	0.5	60	6	10	2	0°
8	0	0.3	20	8	15	3	15°
9	0	0.4	40	10	5	1	30°
10	1	0.3	40	6	10	3	30°
11	1	0.4	60	8	15	1	0°
12	1	0.5	20	10	5	2	15°
13	1	0.4	20	6	15	2	30°
14	1	0.5	40	8	5	3	0°
15	1	0.3	60	10	10	1	15°
16	1	0.4	60	6	5	3	15°
17	1	0.5	20	8	10	1	30°
18	1	0.3	40	10	15	2	0°

3.2. The calculation of SNR

Taguchi method is one of the robust design and optimisation methods, which is employed to determine the values of the control factors discretely to reach the optimal value [22]. In the current study, SNR, ANOVA, regression and residual analysis were utilised for data anaylsis. The SNR is the ratio of the input signal strength to the noise strength, which was used to measure the quality characteristics. Generally, there are three categories to calculate SNR, namely larger is preferable, nominal is optimal, and smaller is preferred.

In the current experiment, COP was selected as the evaluation index of quality characteristic. The value of COP reflects the energy utilisation efficiency of the vortex tube. The larger the COP, the higher the energy utilisation efficiency of the vortex tube, and the better the cooling effect.

During the experiment, the quality characteristics are expected to be larger, Eq. (7) calculate:

$$SNR = -10 \times \log_{10}\frac{1}{n}\sum_{i=1}^{n}\frac{1}{y^2} \tag{7}$$

where, n is the number of experiments. Since no repeated experiment was conducted, $n = 1$; y refers to the measured quantity, namely

COP. In this essay, Eq. (7) is applied for the SNR calculation, and the results are showed in Table 4.

In Table 4, the lowest COP value was 0.081 for group 1, while the largest COP value was 0.107 for group 14. The difference between the maximum and minimum COP values indicates that the control factors have a considerable influence on the properties of the vortex tube. Taguchi method believes that the larger the SNR, the smaller the fluctuation, and more close to the standard evaluation [23]. Group 14 had the highest SNR (−19.41), whereas group 1 had the lowest SNR (−21.83). It means that the combination for group 14 has the least fluctuation and its impact on the COP of vortex tube is the highest.

4. Analytical method

4.1. SNR analysis

In order to explore the best influencing control factors and its effect degree, it is necessary to calculate the SNR value of factors at each levels.

To calculate the SNR of the factor that whether rectifier with or without ring (A1). The SNR value of factor A1 is determined by calculating the average of all SNR values with identical parameter levels. The SNR for the first level of the rectifier without ring is calculated by the following formula Eq.(8), named $SNR_{(A1)}$.

$$SNR_{(A1)} = \frac{(SNR)_1 + (SNR)_2 + \ldots + (SNR)_9}{9} \tag{8}$$

where $(SNR)_1$ is the SNR for group 1, and $(SNR)_2$ is the SNR for group 2. Similarly, to calculate the SNR of P_1, the following equation can be expressed:

$$SNR_{(P1)} = \frac{(SNR)_1 + (SNR)_5 + (SNR)_8 + (SNR)_{10} + (SNR)_{15} + (SNR)_{18}}{6} \tag{9}$$

It is noted that the SNR value of other parameters can also be obtained through these equations. The results have been calculated and exhibited in Table 5, and the main effect diagram was generated according to the calculated SNR are in Fig. 4.

The effect of various parameters on COP can be obtained from the main effect diagram of SNR. Compare the main effect diagram in Fig. 4 and the difference between the maximum and minimum values of SNR in Table 6, it can be inferred that the most important control factor for COP is the length of the rectifier blade, whereas the least control factor is the height of the rectifier. Moreover, the significance of the factors that affect the COP of vortex tube can be ordered as: 1. the length of rectifier blade, 2. inlet pressure, 3. the rectifier with or without ring, 4. distance between the rectifier and the hot end, 5. blades inclination, 6. blades number, and 7. rectifier height.

From the highest point of each control factor effect diagram in Fig. 4, it can be concluded that the optimal combination affecting COP of vortex tube is "A = 1-P = 0.5-S = 20-N = 8-H = 10-L = 3-θ = 30°" (A_2-P_3-S_1-N_2-H_2-L_3-θ_3).

4.2. ANOVA

ANOVA is utilised to test the adequacy of the model. This approach is highly valued in assessing the degree of influence that factors or factor interactions have on a specific response variable [21]. Table 6 depicts the results of the ANOVA and some calculation parameters of Taguchi method. These parameters include the degree of freedom (DF), sum of squares (SS), mean squares (MS), statistical value (F), probability value (P) and the contribution value of each factor to the error variation (C%). The data in the table can be deduced and calculated by following Eqs. (10)–(20) [24].

Calculation of DF：

Table 4
Experimental results of L18 orthogonal array of COP and SNR.

Order	COP	SNR
1	0.081	−21.83
2	0.095	−20.45
3	0.102	−19.83
4	0.085	−21.41
5	0.093	−20.63
6	0.100	−20.00
7	0.090	−20.92
8	0.093	−20.63
9	0.082	−21.72
10	0.096	−20.35
11	0.087	−21.21
12	0.104	−19.66
13	0.100	−20.00
14	0.107	−19.41
15	0.090	−20.92
16	0.101	−19.91
17	0.104	−19.66
18	0.084	−21.51

Table 5
Main effect table of SNR for COP.

Level	A	P (MPa)	S(mm)	N	H(mm)	L(mm)	θ(°)
1	20.82	20.98	20.30	20.74	20.53	21.12	20.81
2	20.29	20.55	20.81	20.33	20.38	20.53	20.50
3		20.15	20.57	20.61	20.77	20.02	20.37
Max-Min	0.53	0.83	0.51	0.41	0.38	1.10	0.45
Rank	3	2	4	6	7	1	5

Note: The values of the SNR are all negative in Table 5.

Fig. 4. Main effect diagram of SNR.

Table 6
ANOVA for SNR of COP.

Source	DF	SS	MS	F	P	C%	Order
A	1	1.2643	1.2643	9.924	0.034506	0.128	3
P	2	2.0676	1.0338	8.115	0.039096	0.210	2
S(mm)	2	0.7812	0.3906	3.066	0.155858	0.079	4
N	2	0.5268	0.2634	2.068	0.241712	0.053	6
H(mm)	2	0.4644	0.2322	1.823	0.273685	0.047	7
L(mm)	2	3.6365	1.8183	14.272	0.015107	0.369	1
θ	2	0.6132	0.3066	2.407	0.205956	0.062	5
Error	4	0.5099	0.1274			0.052	
Total	17	9.8639				1	

A-factor degree of freedom:

$$DF_A = r - 1 \tag{10}$$

The total of DF:

$$DF_T = r - 1 \tag{11}$$

Error degree of freedom:

$$DF_E = DF_T - (DF_A + DF_P + \ldots + DF_\theta) \tag{12}$$

Calculation of sum of squares:
The total sum of squares:

$$TSS = \sum_{i=1}^{n} (y_i - \bar{y})^2 \tag{13}$$

The sum squares of A:

$$SS_A = \sum_{i=1}^{r} m_i (y_i - \overline{y})^2 \tag{14}$$

Total error sum:

$$SSE = TSS - (SS_A + SS_P + \ldots + SS_\theta) \tag{15}$$

Calculation of mean square:

$$MS_A = SS_A / DF_A \tag{16}$$

$$MS_E = SSE / DF_E \tag{17}$$

Calculation of statistical value:

$$F = MS_A / MS_E \tag{18}$$

Contribute%:

$$C\% = SS_A / TSS \tag{19}$$

The probability value:

$$FDIST(F_A, DF_A, DF_E) \tag{20}$$

where, n is the number of the experiments; y_i is the SNR in Table 4; r is the levels number; m_i is the number of the repeated experiments at the level of i, and $\overline{y}$ is the average SNR. The results are given in Table 6.

Under the same cold flow ratio (α = 0.5), the probability value of A, P and L were observed to be less than 0.05 ($P < 0.05$), indicating that the influence of these control factors on the COP of the vortex tube is statistically significant. Moreover, the comparison of F-value with the relevant F-test table shows that the F-value of A, P and L are all greater than 6.61($F > 6.61$ [19]), which suggest that the three control factors have the greatest influence on error variation and are the most important. Meanwhile, it can be intuitively seen from the C% and the ranking in the ANOVA table that the most important control factors on COP is the length of rectifier blade (36.9%), followed by blade number (5.3%), rectifier with or without ring (12.8%), distance between rectifier and hot end (7.9%), blade inclination angle (6.2%), inlet pressure (21%) and rectifier height (4.7%). The test results of the model are consistent with the previous SNR results (Table 5), which verifies the rationality of the ANOVA.

4.3. Regression analysis

Regression analysis is an effective statistical method, which can establish an appropriate functional relationship between the response values and design variables [25]. The linear relationship between the response value and each control factors are as Eq. (21):

$$Y = C + \beta_1 A + \beta_2 P + \beta_3 S + \beta_4 N + \beta_5 H + \beta_6 L + \beta_7 \theta \tag{21}$$

where, Y is the predicted of COP, C is constant term, β_1-β_7 is the regression coefficient of each control factor, and A, P, S, N, H, L, θ are the control factors. In the current study, the correlation coefficient of regression statistics, the residual coefficient of ANOVA, the regression coefficient and the prediction value were obtained as shown in Tables 7–9.

In the regression analysis, R represents the correlation coefficient, and its value range is [−1,1]. If the absolute value of R is closer to 1, it indicates that the linear relationship between the two variables of response value and control factor is stronger. When $|R| \geq 0.8$, it means the two value are highly correlated [26]. In Table 7, R = 0.9082, indicating that there is a strong linear correlation between control factors and the response value COP. The determination coefficient (R^2) is 0.8249, which proves that there is a strong relationship between the quality characteristics and control factors.

The ANOVA of the regression Eq. (21) is resented in Table 8, the regression DF is 7, representing 7 control factors variables. The SS is 0.0009, which represents the total deviation of predicted value of COP from its average value. The residual SSE is 0.0002, which accounts for 17.5% of the total deviation value, indicating that the prediction effect is relatively good. And F value is 6.729. Therefore, it can be confirmed that the prediction equation aligns with the test results, which indicates a stronger level of significance. Table 9 also gives the probability value of A, P and L. All of them are less than 0.05 through the regression analysis, which is consistent with the

Table 7
Regression statistical results.

Regression statistical	
Multiple R	0.908233
R Square	0.824887
Adjusted R	0.702309
Standard error	0.00446
Observed value	18

Table 8
ANOVA of the regression equation.

	DF	SS	MS	F	P
Regression Analysis	7	0.000937	0.000134	6.729449	0.003912
Residual	10	0.000199	1.99×10^{-5}		
Total	17	0.001136			

Table 9
The Coefficients measure of regression.

Tern	Coefficients	standard error	t Stat	P-value	Upper 95.0%	Under 95.0%
	0.061889	0.008763	7.062383	3.45E-05	0.042363	0.081414
A	0.005778	0.002102	2.748285	0.020539	0.001094	0.010462
P	0.045833	0.012874	3.560138	0.00518	0.017148	0.074518
S	−7.9E-05	6.44E-05	−1.22987	0.246896	−0.00022	6.43E-05
N	0.000375	0.000644	0.582568	0.573085	−0.00106	0.001809
H	−0.00028	0.000257	−1.10041	0.296938	−0.00086	0.00029
L	0.005833	0.001287	4.531084	0.00109	0.002965	0.008702
θ	0.000156	8.58E-05	1.812434	0.100004	−3.6E-05	0.000347

previous conclusion (Table 6). The regression Eq. (22) was obtained by substituting the regression coefficient into Eq. (21).

$$COP = 0.06188 + 0.005778A + 0.045833P - 7.9 \times 10^{-5}S + 0.000375N - 0.00028H + 0.005833L + 0.000156\theta \quad (22)$$

4.4. Residual analysis

The residual normal probability graph was used to test whether the residual conforms to normal distribution, as shown in Fig. 5. Table 10 is the output results of the residual. As shown in Fig. 5, with the increase of the fitting value, all observation points fluctuate up and down the central line, and the fluctuation range is very small. Therefore, the residual error conforms to normal test.

5. Prediction of optimal value

5.1. Optimal prediction

It can be seen from section 3.1 that the optimal combination is A_2-P_3-S_1-N_2-H_2-L_3-θ_3. In order to verify the accuracy of the optimal value predicted by Taguchi method, a new vortex tube and a rectifier were fabricated according to the predicted results. The predicted value of COP can be obtained by substituting the optimal level parameters into Eqs. (22) and (1), $COP_{(P)} = 0.112$, $SNR_{(p)} = -19.02$. The optimal experiment value is shown in Table 11, and the comparison between the optimal result and the prediction value is in Table 12.

Using 95% CI to evaluate the verification result of the optimal control factor level, and its value is calculated from Eqs. (23) and (24) [20];

$$CI = \sqrt{F_{0,0.5,(1,f_e)} V_e \left(1/\eta_{eff} + 1/r\right)} \quad (23)$$

$$\eta_{eff} = N/1 + \nu_T \quad (24)$$

where, $F_{0,0.5,(1,f_e)}$: error degree of freedom; V_e: error variance; η_{eff}: number of real repetitions; r: number of repetitions for conformation experiments; N: total number of experiments, ν_T: sum of the degree of freedom for control factors. $F_{0,0.5,(1,f_e)} = 6.61$, $V_e = 0.1275$ (Table 6), the experiment was not repeated, r = 1, $\eta_{eff} = 35$. By substituting the above data into Eq. (23), we have CI = ±0.517.

According to Table 12, there is a difference value of −18.50 and −19.54 between the SNR(p) and CI values, respectively, due to the positive and negative value of CI number. As can be seen from the result of Eq. (25). Therefore, the value of SNR ($_{o)}$ (−19.41) is located between the two distinct value, which means the COP value can be accepted as the optimal result.

$$SNR_{(p)} - CI = -19.54 < SNR_{(o)} = -19.41 < SNR_{(p)} + CI = -18.50 \quad (25)$$

The COP value is confirmed and obtained as the optimal values $COP_{(o)} = 0.107$ and $SNR_{(o)} = -19.41$ were determined. In addition, the difference between the SNR $_{(o)}$ and the $SNR_{(p)}$ is 0.39, which is within the range of the value of CI (0.517), the results show that the prediction of the optimal COP is appropriate.

5.2. Comparison between optimal and original combination

According to the above analysis, it was found that the combination of (A2-P3-S1-N2-H2-L3-θ3) shows the highest COP value, which is almost same as that of the original optimum combination (group 14 A2-P3-S2-N2-H1-L3-θ1). Therefore, both combinations need to be further compared and analyzed. Fig. 6 shows the fitting diagram of the two groups of experiment data. From Fig. 6, the value of COP increases rapidly follows by a quick decrease with the increase of the cold flow ratio (α). When α is less than 0.63, the curve of the optimal combination (1-8-10-3-30°) is above the original combination (1-8-5-3-0°). It indicates that the cooling performance of the

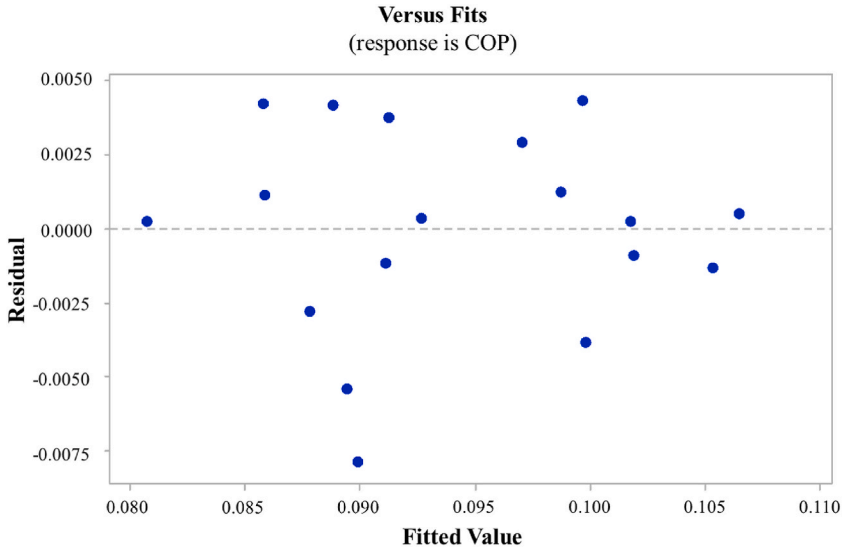

Fig. 5. Residual normal probability diagram.

Table 10
Residual output results.

Text number	Predict Y	Residual
1	0.080722	0.000278
2	0.091222	0.003778
3	0.101722	0.000278
4	0.087806	−0.00281
5	0.088806	0.004194
6	0.097056	0.002944
7	0.091139	−0.00114
8	0.092639	0.000361
9	0.089889	−0.00789
10	0.099833	−0.00383
11	0.085833	0.001167
12	0.105333	−0.00133
13	0.09875	0.00125
14	0.1065	0.0005
15	0.08575	0.00425
16	0.101917	−0.00092
17	0.099667	0.004333
18	0.089417	−0.00542

Table 11
Optimal experiment of COP.

A	P(MPa)	S(mm)	N	H(mm)	L(mm)	θ	$COP_{(o)}$	$SNR_{(o)}$
1	0.5	20	8	10	3	30	0.107	−19.41

Table 12
Comparison between optimal experiment value and predicted.

Optimal result		Predicted parameters		Difference	
$COP_{(o)}$	$SNR_{(o)}$	$COP_{(p)}$	$SNR_{(p)}$	$\lvert COP_{(o)}\text{-}COP_{(p)}\rvert$	$\lvert SNR_{(o)}\text{-}SNR_{(p)}\rvert$
0.107	−19.41	0.112	−19.02	0.005	0.39

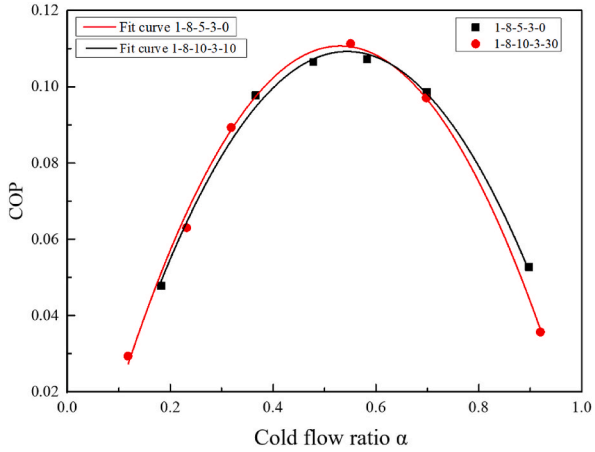

Fig. 6. Comparison of COP between optimal result and original.

optimal combination is higher to the original combination at small α. It can also be seen that the COP of the optimal combination reaches the peak value (0.1112) at α of 0.53. It indicates that the prediction of optimal value is valid and reliable.

6. Conclusions

In the current study, the feasibility of the predicted optimisation method for achieving the optimal combination of COP in the vortex tube was determined through the application of SNR, ANOVA, regression, and residual analysis. The experimental results have successfully demonstrated the effectiveness of the proposed optimisation method, leading to the following main conclusions:

(1) The variation in COP values, which are considered as the quality characteristics, indicates that the rectifier structure can play an important role in influencing the COP of the vortex tube. The most optimal combination for the COP of the vortex tube is: A = 1; P = 0.5 MPa; S = 20 mm; N = 8; H = 10 mm; L = 3 mm; and θ = 30°.
(2) The probability value for A, P, and L is smaller than 0.05, indicating that the effect of these control factors on the quality characteristics (COP) of the vortex tube is statistically significant.
(3) The current work reveals that the values of COP were mostly influenced by the length of rectifier blade (36.9%), followed by blade number (5.3%), rectifier with or without ring (12.8%), distance between rectifier and the hot end (7.9%), the inclination angle of blades (6.2%), inlet pressure (21%) and the height of rectifier (4.7%);
(4) The determination coefficient $R^2 = 82.49\%$ was obtained by regression analysis, which indicates that there is a significant linear relationship between the control factors and the COP.

Author statement

Zhuohuan Hu: Experimental Design; Methodology; Data Analysis; Draft writing.
Dan Wang: Experimental setup and Calculation.
Fan Gao: Experimental setup.
Yan Cao: Test and data analysis.
Hongwei Wu: Conceptualization; Discussion; Supervision.

Declaration of competing interest

The authors declare that they have no known competing financial interests or personal relationships that could have appeared to influence the work reported in this paper.

Data availability

Data will be made available on request.

Acknowledgments

This work is supported in part by HORIZON-MSCA-2021-SE-01 (No.101082394).

References

[1] J. Zhu, X. Xiang, X. Hu, C. Xia, Effects of tip clearance height on hot-streak migration in high subsonic micro turbine[J], Case Stud. Therm. Eng. 42 (2023), 102703, https://doi.org/10.1016/j.csite.2023.102703.

[2] B. Zhang, X. Guo, Prospective applications of Ranque-Hilsch vortex tubes to sustainable energy utilization and energy efficiency improvement with energy and mass separation[J], Renew. Sustain. Energy Rev. 89 (2018) 135–150, https://doi.org/10.1016/j.rser.2018.02.026.
[3] H. Peng, G. Xiangji, Numerical study on the cooling performance and inlet mass flow rate per unit area of Ranque-Hilsch Vortex tubes with different area ratios [J], Numer. Heat Tran. Part A: Appl. 136 (2023) 287–292, https://doi.org/10.1080/10407782.2022.2156946.
[4] T.K. Sharma, G.A.P. Rao, K.M. Murthy, Numerical analysis of a vortex tube: a review[J], Arch. Comput. Methods Eng. 24 (2017) 251–280, https://doi.org/10.1007/s11831-016-9166-3.
[5] X. Guo, B. Zhang, Y. Shan, LES study on the working mechanism of large-scale precessing vortices and energy separation process of Ranque-Hilsch vortex tube [J], Int. J. Therm. Sci. 163 (2021), 106818, https://doi.org/10.1016/j.ijthermalsci.2020.106818.
[6] J. Yun, Y. Kim, S. Yu, Feasibility study of carbon dioxide separation from gas mixture by vortex tube[J], Int. J. Heat Mass Tran. 126 (2018) 353–361, https://doi.org/10.1016/j.ijheatmasstransfer.2018.04.150.
[7] A. Aghagoli, M. Sorin, Thermodynamic performance of a CO_2 vortex tube based on 3D CFD flow analysis[J], Int. J. Refrig. 108 (2019) 124–137, https://doi.org/10.1016/j.ijrefrig.2019.08.022.
[8] H. Kandil, S. Abdelghany, Computational investigation of different effects on the performance of the Ranque–Hilsch vortex tube[J], Energy 84 (2015) 207–218, https://doi.org/10.1016/j.ijrefrig.2017.09.010.
[9] F. Liang, Q. Zeng, G. Tang, et al., Numerical investigation on the effect of convergent-divergent tube on energy separation characteristic of vortex tube[J], Int. Commun. Heat Mass Trans. 133 (2022), 105927, https://doi.org/10.1016/j.icheatmasstransfer.2022.105927.
[10] A. Celik, M. Yilmaz, M. Kaya, S. Karagoz, The experimental investigation and thermodynamic analysis of vortex tubes[J], Heat Mass Tran. 53 (2017) 395–405, https://doi.org/10.1007/s00231-016-1825-2.
[11] M. Parker, A. Straatman, Experimental study on the impact of pressure ratio on temperature drop in a Ranque-Hilsch vortex tube[J], Appl. Therm. Eng. 189 (2021), 116653, https://doi.org/10.1016/j.applthermaleng.2021.116653.
[12] S.Y. Khan, U. Allauddin, S.M.F. Hasani, R. Khan, M. Arsalan, A CFD analysis on the effect of tube curvature, hot flow control valve profile, and inlet swirl on the thermal performance of curved vortex tubes[J], J. Therm. Anal. Calorim. 147 (2022) 12761–12778, https://doi.org/10.1007/s10973-022-11479-1.
[13] P. Ambedkar, T. Dutta, Analysis of various separation characteristics of Ranque-Hilsch vortex tube and its applications – a review[J], Chem. Eng. Res. Des. (2023) 93–108, https://doi.org/10.1016/j.cherd.2023.01.019.
[14] R. Godbole, P. Ramakrishna, Design guidelines for the Vortex tube[J], Exp. Therm. Fluid Sci. 118 (2020), 110169, https://doi.org/10.1016/j.expthermflusci.2020.110169.
[15] O. Vitovsky, Experimental study of energy separation in a Ranque-Hilsch tube with a screw vortex generator[J], Int. J. Refrig. 126 (2021) 272–279, https://doi.org/10.1016/j.ijrefrig.2021.02.014.
[16] V. Kirmaci, H. Kaya, Effects of working fluid, nozzle number, nozzle material and connection type on thermal performance of a ranque-hilsch vortex tube: a review[J], Int. J. Refrig. 118 (2018), 110169, https://doi.org/10.1016/j.ijrefrig.2018.05.005.
[17] M. Suhaimi, L. Hong, M. Yusof, Experimental study on the performance of vortex tube cooling device on a cooling jacket[J], IOP Conf. Ser. Earth Environ. Sci. 581 (2020), 012018, https://doi.org/10.1088/1755-1315/581/1/012018.
[18] G. Kumar, G. Padmanabhan, B. Sarma, Optimizing the temperature of hot outlet air of vortex tube using Taguchi method[J], Procedia Eng. 97 (2014) 828–836, https://doi.org/10.1016/j.proeng.2014.12.357.
[19] H. Kaya, Evaluation of performance of parallel connected vortex tubes using air, oxygen and carbon dioxide with Taguchi method[J], Heat Mass Tran. 57 (2020) 165–174, https://doi.org/10.1007/s00231-020-02968-w.
[20] H. Gokce, Optimization of Ranque-Hilsch vortex tube performances via Taguchi method[J], J. Braz. Soc. Mech. Sci. Eng. 42 (2020) 558, https://doi.org/10.1007/s40430-020-02649-z.
[21] A. Sarifudin, D. Wijayanto, I. Widiastuti, Parameters optimization of tube type, pressure, and mass fraction on vortex tube performance using the Taguchi method[J], Int. J. Heat Technol. 37 (2019) 597–604, https://doi.org/10.18280/ijht.370230.
[22] J. Simões-Moreira, An air-standard cycle and a thermodynamic perspective on operational limits of Ranque–Hilsh or vortex tubes[J], Int. J. Refrig. 33 (2010) 765–773, https://doi.org/10.1016/j.ijrefrig.2010.01.005.
[23] P. Yang, H. Zhang, Y. Zheng, Z. Fang, X. Shi, Y. Liu, Investigation and optimization of heat transfer performance of a spirally corrugated tube using the Taguchi method[J], Int. Commun. Heat Mass Tran. 127 (2021), 105577, https://doi.org/10.1016/j.icheatmasstransfer.2021.105577.
[24] X. Lin, Taguchi Method Actual Combat Technology [M], Haitian Publishing House, 2004.
[25] J. Hu, Y. Kang, Y. Lu, J. Yu, K. Zhong, Simplified models for predicting thermal stratification in impinging jet ventilation rooms using multiple regression analysis[J], Build. Environ. 206 (2021), 108311, https://doi.org/10.1016/j.buildenv.2021.108311.
[26] M. Ling, L. Tan, Y. Liu, Basic Statistics, fifth ed., Higher Education Press, Beijing, 2018, pp. 161–165 [M].